Mesoscale Eddies Drive Increased Silica Export in the Subtropical Pacific Ocean

Claudia R. Benitez-Nelson, *et al.*

Science **316**, 1017 (2007);
DOI: 10.1126/science.1136221

combined with the action of flow (which orients the tethered long chains much more than the rest) can explain why long chains enhance shish propagation (*11*). The elevated orientation created near the shish causes rapid ordering.

It has been shown that during flow, shish can increase in length by micrometers per second (*26*). The time it takes for a shish to overtake a typical long- or medium-length chain ($\Delta t \approx$ 1 ms) is too fast for its center of mass to diffuse out of or into the path of propagation. In Δt = 1 ms, even a medium-length chain of 200 kg/mol chain diffuses less than 1 nm; i.e., $(D\,\Delta t)^{1/2} <$ 1 nm (*29*). There simply is not enough time to segregate the long chains from the bulk into the shish. Thus, long chains greatly enhance the propagation velocity of shish, with the kinetic consequence that all lengths of chains become incorporated as the shish advances.

Direct measurement of chains of different lengths partitioning into the shish shows that the fraction of long-chain segments within the shish matches their composition in the melt as a whole. This finding is consistent with previous literature showing that the longest chains play a central role in the formation of shish. The two observations taken together indicate that the long chains recruit neighboring chains to join them in forming the shish. The physical picture is consistent with the observations of Rutledge and co-workers in their simulations of nucleation from the melt: Molecular mobility and relaxation of a number of neighboring segments into crystalline-like order is vital to the formation of nuclei from an oriented melt (*30*).

The implications of molecular-level understanding of the formation of the highly oriented morphology in semicrystalline polymers are widespread. Judicious choice of the concentration and length of long chains can be used to tune the properties of the oriented skin that are vital to applications ranging from biomedicine to transportation: Surface hardness, impact resistance, reflectivity, and adhesion, among many other qualities, depend upon the microstructure near the surface. The realization that shish formation involves all chain lengths underscores the potential for further expansion of the diversity of material properties that can be achieved using the same basic set of monomers.

References and Notes

1. C. Vasile, Ed., *Handbook of Polyolefins* (Dekker, New York, ed. 2, 2000).
2. Z. Bashir, J. A. Odell, A. Keller, *J. Mater. Sci.* **21**, 3993 (1986).
3. G. W. Coates, R. M. Waymouth, *Science* **267**, 217 (1995).
4. D. J. Arriola, E. M. Carnahan, P. D. Hustad, R. L. Kuhlman, T. T. Wenzel, *Science* **312**, 714 (2006).
5. Z. Guan, P. M. Cotts, E. F. McCord, S. J. McLain, *Science* **283**, 2059 (1999).
6. K. Kageyama, J. Tamazawa, T. Aida, *Science* **285**, 2113 (1999).
7. A. Keller, H. W. H. Kolnaar, in *Materials Science and Technology*, vol. 18 of *Processing Polymers*, H. E. H. Meijer, Ed. (Wiley VCH, New York, 1997), pp. 189–268.
8. S. Mitsuhashi, *Bull. Text. Res. Inst.* **66**, 1 (1963).
9. A. J. Pennings, A. M. Kiel, *Kolloid Z. Z. Polym* **205**, 160 (1965).
10. F. L. Binsbergen, *Nature* **211**, 516 (1966).
11. M. Seki, D. W. Thurman, J. P. Oberhauser, J. A. Kornfield, *Macromolecules* **35**, 2583 (2002).
12. H. Janeschitz-Kriegl, E. Ratajski, M. Stablbauer, *Rheol. Acta* **42**, 355 (2003).
13. L.-B. Li, W. H. de Jeu, *Macromolecules* **36**, 4862 (2003).
14. I. Dukovski, M. Muthukumar, *J. Chem. Phys.* **118**, 6648 (2003).
15. A. Elmoumni, H. H. Winter, A. J. Waddon, *Macromolecules* **36**, 6453 (2003).
16. B. A. G. Schrauwen *et al.*, *Macromolecules* **37**, 8618 (2004).
17. M. Wang, W. Hu, Y. Ma, Y.-Q. Ma, *Macromolecules* **38**, 2806 (2005).
18. B. S. Hsiao, L. Yang, R. H. Somani, C. A. Avila-Orta, L. Zhu, *Phys. Rev. Lett.* **94**, 117802 (2005).
19. D. P. Pope, A. Keller, *Colloid Polym. Sci.* **256**, 751 (1978).
20. M. J. Miles, A. Keller, *Polymer* **21**, 1295 (1980).
21. A. Keller, J. A. Odell, *Nature* **312**, 98 (1984).
22. A. Nogales *et al.*, *Polymer* **42**, 5247 (2001).
23. Materials and methods are available as supporting material on *Science* Online.
24. W. Wiyatno *et al.*, *Macromolecules* **36**, 1178 (2003).
25. G. Kumaraswamy, A. Issaian, J. K. Kornfield, *Macromolecules* **32**, 7537 (1999).
26. J. A. Kornfield, G. Kumaraswamy, A. M. Issaian, *Ind. Eng. Chem. Res.* **41**, 6383 (2002).
27. S. K. Ghosh, M. Hikosaka, A. Toda, S. Yamazaki, K. Yamada, *Macromolecules* **35**, 6985 (2002).
28. D. G. H. Ballard, P. Cheshire, W. Longman, *Polymer* **19**, 379 (1978).
29. J. van Meerveld, *Rheol. Acta* **43**, 615 (2004).
30. M. S. Lavine, N. Waheed, G. C. Rutledge, *Polymer* **44**, 1771 (2003).

31. This work was performed using SANS-U of the Institute for Solid State Physics, the University of Tokyo (no. 05.5542). Supported by the NSF Division of Materials Research (DMR-0505393 and Materials Research Science and Engineering Center DMR-0080065).

Supporting Online Material

www.sciencemag.org/cgi/content/full/316/5827/1014/DC1
Materials and Methods
SOM Text
Figs. S1 to S7
Tables S1 and S2
References

19 January 2007; accepted 23 March 2007
10.1126/science.1140132

Mesoscale Eddies Drive Increased Silica Export in the Subtropical Pacific Ocean

Claudia R. Benitez-Nelson,[1]* Robert R. Bidigare,[2] Tommy D. Dickey,[3] Michael R. Landry,[4] Carrie L. Leonard,[5] Susan L. Brown,[2] Francesco Nencioli,[3] Yoshimi M. Rii,[2] Kanchan Maiti,[1] Jamie W. Becker,[6] Thomas S. Bibby,[7,8] Wil Black,[3] Wei-Jun Cai,[9] Craig A. Carlson,[10] Feizhou Chen,[9] Victor S. Kuwahara,[3,11] Claire Mahaffey,[2] Patricia M. McAndrew,[2] Paul D. Quay,[12] Michael S. Rappé,[6] Karen E. Selph,[2] Melinda P. Simmons,[4,13] Eun Jin Yang[4,14]

Mesoscale eddies may play a critical role in ocean biogeochemistry by increasing nutrient supply, primary production, and efficiency of the biological pump, that is, the ratio of carbon export to primary production in otherwise nutrient-deficient waters. We examined a diatom bloom within a cold-core cyclonic eddy off Hawai`i. Eddy primary production, community biomass, and size composition were markedly enhanced but had little effect on the carbon export ratio. Instead, the system functioned as a selective silica pump. Strong trophic coupling and inefficient organic export may be general characteristics of community perturbation responses in the warm waters of the Pacific Ocean.

Mesoscale eddies in the world's oceans are ubiquitous and bring episodic pulses of new nutrients into the photic zone. Their ephemeral nature, however, makes them difficult to study (*1*), and their biogeochemical importance remains controversial (*2*, *3*). The E-Flux project was designed to exploit the reliable presence of one type of commonly occurring wind-driven mesoscale eddy that forms in the lee of the Hawaiian Islands (*4*, *5*). This region thus serves as a natural laboratory for investigating eddy-enhanced production and particle export in an oligotrophic subtropical ecosystem (*1*, *6*–*8*). Here, we report the physical and biogeochemical dynamics of a first baroclinic mode eddy, Cyclone Opal, which became visible in Moderate Resolution Imaging Spectroradiometer (MODIS) and Geostationary Operational Environmental Satellite (GOES) imagery between 18 and 25 February 2005.

Cyclone Opal appears to have originated between the islands of Maui and Hawai`i because of strong and persistent northeasterly trade winds. Under these conditions, the wind stress curl drives Ekman pumping, leading to doming of isopycnal surfaces (*4*, *5*). Shipboard measurements (10 to 22 March) confirmed that Cyclone Opal was a well-developed cold-core eddy as evidenced by its size, tangential current speeds, vertical isopycnal displacements, and outcroppings of density and nutrient surfaces (Figs. 1 and 2). Within this feature, a core region of high biomass that supported euphotic zone primary production (PP) (*9*) rates two- to threefold higher than surrounding oligotrophic waters (Table 1) was confined to an area less than 40 km in diameter. A strongly developed diatom bloom occurred in the deep chlorophyll maximum (DCM) of the eddy's core isopycnal surfaces (σ_t = 24.2 to 24.4 kg m^{-3}) that had been uplifted to 60- to 80-m depth. Cyclone Opal was tracked by a shipboard acoustic Doppler current profiler as it moved ~165 km

southward with an average translational speed of 8 km day^{-1}. Although the eddy maintained its primary physical features and mesoscale structure throughout these observations, the biogeochemistry of the core region evolved substantially. Cyclone Opal therefore provided an intriguing glimpse into a nutrient-perturbed oceanic community entering its biologically declining phase.

The biological community within Cyclone Opal was vertically heterogeneous, with a strong subsurface diatom bloom superimposed onto a typical oligotrophic community of smaller photoautrophic cells (Fig. 2 and Table 1). Initially, large (>20 μm) diatoms in the DCM were enhanced by almost 100-fold above background levels, with a 60-fold increase in the biomarker fucoxanthin (Fig. 3). Diatoms also composed 78% of the highest biomass observed in Cyclone Opal (89 μg C l^{-1}, Fig. 3), with about half attributed to two centric genera, *Rhizosolenia* and *Chaetoceros*. In contrast, DCM communities outside the eddy were dominated by small autotrophs (80% of biomass had cells <10-μm), such as prymnesiophytes, pelagophytes, and *Prochlorococcus* spp. In general appearance as well as total biomass and size composition, Cyclone Opal's bloom bore a striking similarity to the iron-induced bloom observed during the Southern Ocean Iron Experiment (*10*). Cyclone Opal was notably not dominated by pennate diatoms, as occurred in iron-fertilized equatorial waters (*11*).

Contributing to the vertical heterogeneity within Cyclone Opal was a distinct and persistent layer of decaying and senescent diatom cells directly above the DCM. Epifluorescence microscopy indicated that ~90% of these cells were lacking in chlorophyll and/or cellular protein, and fast repetition rate fluorometry (FRRF) indicated that photochemical energy conversion efficiency was depressed [variable fluorescence/maximal fluorescence (F_v/F_m) = 0.34 at 50 to 60 m versus 0.49 at 70 to 80 m]. These differences in diatom physiological state suggest that the bloom began as nutrients were uplifted into lit surface waters and then declined because of nutrient limitation. This decline enabled light penetration and diatom growth to extend to deeper waters.

Cyclone Opal's biological evolution was readily apparent from 16 to 21 March. Daily observations within the DCM showed an 80% decrease in diatom biomass and a 70% decrease in fucoxanthin (Fig. 3). During this period, the diatom assemblage transitioned to lightly silicified genera *Hemiaulus* and *Mastogloia* and smaller pennate forms more common in surrounding waters (*12*). These community changes were accompanied by a gradual DCM decline in F_v/F_m (from 0.51 to 0.41), and the light-limited rate of photosynthesis decreased from 0.07 to 0.04 [mg C mg chlorophyll a (chl a)$^{-1}$ hour^{-1}] (mmol quanta m^{-2} s^{-1})$^{-1}$. These results are consistent with a transition in plankton community metabolism from net autotrophy to heterotrophy (*9*).

We investigated plankton growth and grazing during this decline (*9*). Diatom growth rate was indistinguishable between eddy core and surrounding waters when integrated over the entire euphotic zone. However, there was substantial depth variability within Cyclone Opal, with highest diatom growth at the DCM [0.57 ± 0.18 day^{-1} (mean ± SD) at 70 to 80 m; n = 6 measurements] and the lowest diatom growth directly above at 50 to 60 m (0.23 ± 0.25 day^{-1} at 50 to 60 m; n = 9), corresponding to healthy and senescent diatom layers, respectively. Substantial net diatom growth only occurred in the DCM (0.26 ± 0.12 day^{-1}; n = 6) yet was accom-

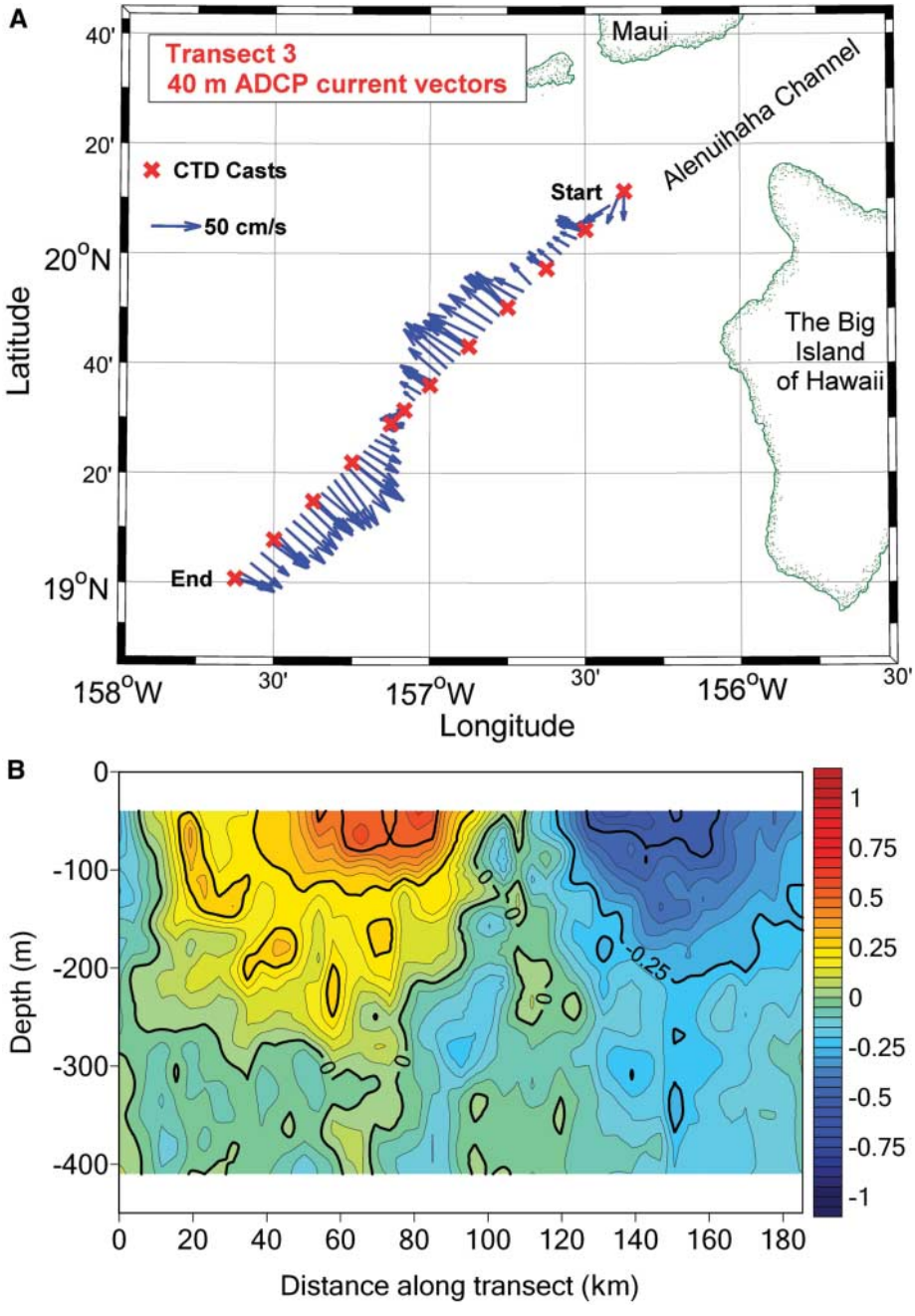

Fig. 1. Spatial distribution of the areal extent of Cyclone Opal during transect 3 as depicted by (**A**) 40-m current vectors and (**B**) sectional perpendicular velocities (m s^{-1}).

[1]Department of Geological Sciences and Marine Science Program, University of South Carolina, Columbia, SC 29208, USA. [2]Department of Oceanography, University of Hawai'i at Manoa, Honolulu, HI 96822, USA. [3]Ocean Physics Laboratory, University of California at Santa Barbara, Goleta, CA 93117, USA. [4]Scripps Institution of Oceanography, University of California at San Diego, La Jolla, CA 92093–0227, USA. [5]BAE Systems, S2 Identification and Surveillance, Honolulu, HI 96813, USA. [6]Hawai'i Institute of Marine Biology, University of Hawai'i, Kaneohe, HI 96744, USA. [7]National Oceanography Center, University of Southampton, Southampton SO14 3ZH, UK. [8]Institute of Marine and Coastal Sciences, Rutgers University, New Brunswick, NJ 08901, USA. [9]Department of Marine Sciences, University of Georgia, Athens, GA 30602–3636, USA. [10]Department of Ecology, Evolution, and Marine Biology, University of California at Santa Barbara, Santa Barbara, CA 93106–9610, USA. [11]Faculty of Education, Soka University, Tokyo 192-8577, Japan. [12]School of Oceanography, University of Washington, Seattle, WA 98195–5351, USA. [13]Gordon and Betty Moore Foundation, San Francisco, CA 94129–0910, USA. [14]Marine Environment Research Department, Korea Ocean Research and Development Institute, Seoul 425-600, South Korea.

*To whom correspondence should be addressed. E-mail: cbnelson@geol.sc.edu

panied by higher diatom mortality by microherbivore grazing (0.31 ± 0.26 day^{-1} versus 0.21 ± 0.14 day^{-1}). In contrast, within the senescent diatom zone, grazing losses yielded negligible net diatom growth (0.02 ± 0.20 day^{-1}; $n = 9$).

On the basis of these experiments, it appears that reduced growth rate rather than a grazing surge precipitated diatom demise, which is consistent with observed distributions of senescent and healthy cells. Although the ultimate cause of diatom decline remains elusive, it may be due to silicic acid limitation. The ratio of silica (Si) to nitrogen (nitrate plus nitrite, N+N) availability was strongly depressed in the eddy core (Table 1). In the senescent zone, silicic acid concentrations were below detection (<0.35 μM) during initial sampling. Furthermore, in a series of experiments under simulated in situ conditions, phytoplankton from the eddy core DCM did not respond to varying combinations of added nitrate, phosphate (P), and iron (*9*). In contrast, experiments in surrounding waters showed a strong and rapid recovery response of F_v/F_m in all nitrate addition treatments, implying nitrate limitation. Taken in combination, low concentrations of silicic acid and the lack of phytoplankton community response to additions of nitrate, P, and iron strongly suggest that DCM populations were Si-limited.

We then considered a hypothetical upper limit to organic carbon export efficiency where all new nutrients (N+N) lifted into the sunlit layer are eventually returned to depth as organic particles with an assumed canonical Redfield C/N ratio of 6.6. The contribution of new production that could be attributed to bloom decline was determined through a salt budget based on uplifted isopycnal density surfaces within the eddy core (*9*). About 147 ± 32 mmol m^{-2} of N+N was initially brought into the euphotic zone (Table 1). If all uplifted N+N were used by phytoplankton, the potential new production during the roughly 4- to 5-week lifetime of Cyclone Opal is equivalent to half of the annual new production in this region [2.0 mol C m^{-2} year^{-1} above 100 m (*13*)] and is almost 10 times higher than the amount directly observed (Table 1). We hypothesize that Si limitation of diatoms coupled with enhanced grazing results in efficient C remineralization but enhanced biogenic silica export, consistent with the model proposed by Dugdale *et al.* (*14*) for high-nutrient low-chlorophyll waters.

Microzooplankton consumers accounted for most of the utilization of diatom production, as evidenced by a lack of fecal pellets and denuded diatom frustules. As a consequence, the fate of diatom production was toward remineralized C, N, and P and empty diatom frustules within the euphotic zone, rather than the rapid export of organic-rich large particles, e.g., compacted fecal pellets or aggregates of intact diatoms. Strong microzooplankton grazing relative to macrozooplankton grazing facilitated recycling and greatly diminished the potential for high export ratios of C and associated bio-elements from the wind-driven eddy-stimulated bloom (Table 1).

This hypothesis is further supported by bacterial community composition, total organic carbon (TOC) accumulation, and particulate C (PC) and N (PN) export rates. Mixed layer bacterioplankton communities were similar to those measured outside the eddy. Below 50 m, however, *Planctomycetes*, *Bacteroidetes*, and certain *Proteobacteria* thought to degrade high–molecular weight dissolved organic matter appeared (*15*–*17*). TOC concentrations within the upper 110 m increased by 600 mmol C m^{-2} (expected versus observed, Table 1). In contrast, PC and PN exports were only minimally enhanced within the eddy core (Table 1) and were similar to those in nearby oligotrophic waters at station (Sta.) ALOHA (Hawai`i Ocean time series program) (*13*, *18*).

Collectively, our results suggest that Cyclone Opal was surprisingly inefficient in transporting PC

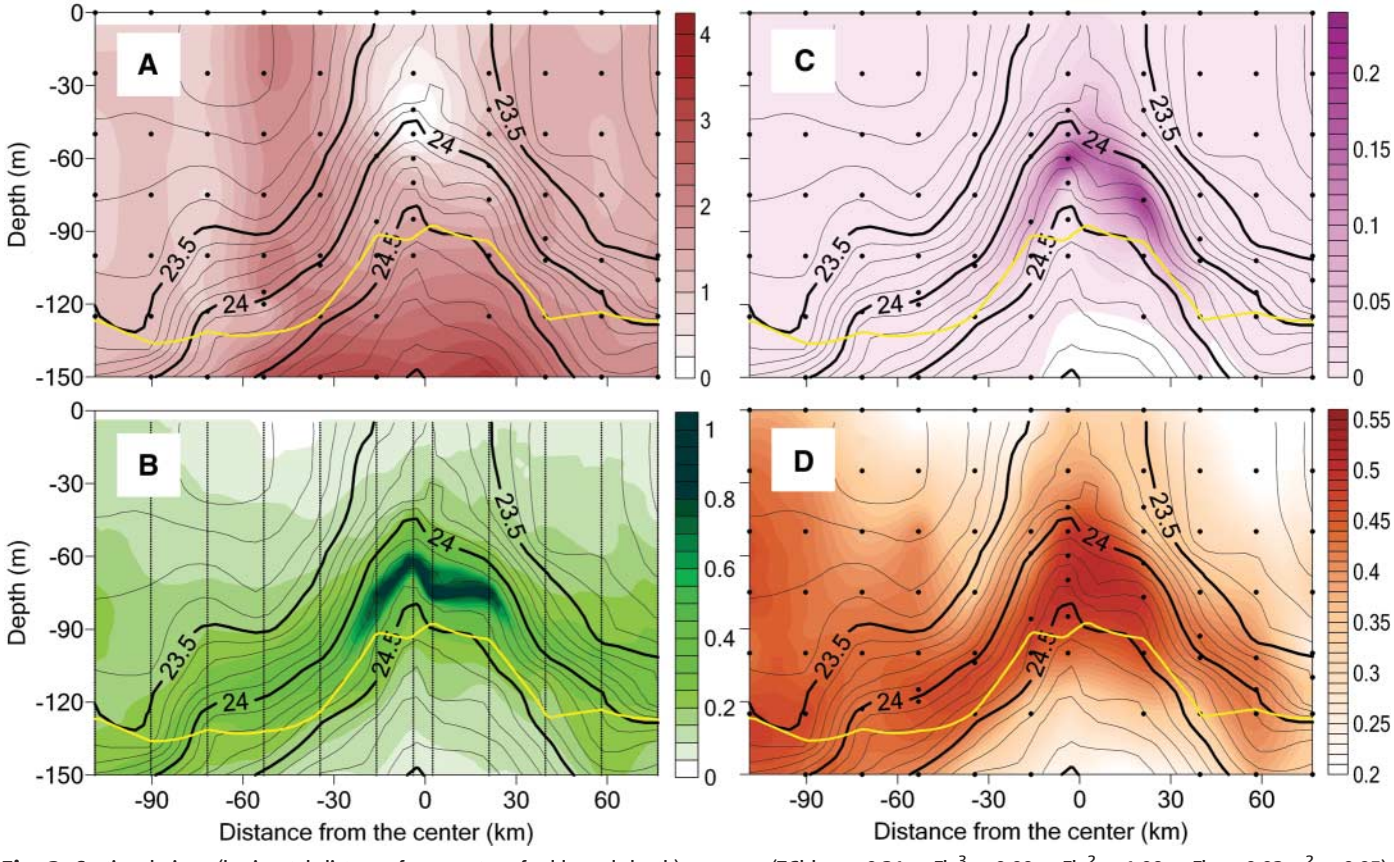

Fig. 2. Sectional views (horizontal distance from center of eddy and depth) for transect 3. Contour lines indicate the depth of isopycnal surfaces: (**A**) silicic acid (μM), (**B**) total chlorophyll a (TChl a, mg m^{-3}), (**C**) fucoxanthin (mg m^{-3}), and (**D**) photochemical energy conversion efficiency (F_v/F_m). TChl a is derived with the relationship between conductivity temperature depth (CTD) fluorometer voltage (Flu) and high-performance liquid chromatography (HPLC)–measured TChl a by using a third-order regression curve (TChl a = $0.31 \times \text{Flu}^3 - 0.80 \times \text{Flu}^2 + 1.09 \times \text{Flu} - 0.02$; $r^2 = 0.85$). The yellow line in each contour represents the 1% light level. The 1% light level depth was computed by using the following relationship: $\log_{10}Z_e = -0.64429(\log_{10}C) + 1.16115$, where Z_e is the 1% light level depth and C is the mean value of the chlorophyll concentration between 0 and Z_e. $\log_{10}Z_e$ and $\log_{10}C$ were first computed for casts collected during daylight hours and interpolated (*29*).

to depth. Although gross PP (GPP) rates were elevated by over a factor of 2, the ratio of PC export to GPP remained low at 0.05, similar to that measured at Sta. ALOHA (*19*) and other open-ocean ecosystems (*20*). More than 85% of net community production (NCP) accumulated as TOC in the water column (Table 1) (*9*). Although this finding is consistent with the pelagic food web model of Laws *et al*. (*21*), which predicts that export ratios do not vary with total production at temperatures greater than ~25°C, the export ratio is substantially less than commonly associated with large-scale diatom blooms (*22*).

Table 1. Water column properties of IN versus OUT stations occupied during the E-Flux III cruise (values in parentheses correspond to the number of observations). Mixed layer depth is defined as the depth at which seawater temperature is 1°C less than the temperature at 10 m. All observed (^{obs}) nutrient data were averaged over the upper 110 m in all control (OUT, $n = 3$) and IN stations ($n = 7$), which include the center station from transect 3 depicted in Fig. 1. Expected nutrient data (^{exp}) for IN stations was determined by using a salt budget based on the isopycnal uplift and compaction of density surfaces (*9*). GPP and NCP calculated from $\Delta^{17}O$ were determined over the depth of the mixed layer. GPP and NCP from $\Delta^{17}O$ were not determined at the OUT station during the March 2005 cruise. As such, average values were used from two previous cruises in November 2004 and January 2005 from the same OUT station location. All biological and pigment data, as well as PP derived from phytoplankton growth, were averaged to depths just below the 1% light level within the eddy core (0 to 110 m, center station from transect 3 and the first three eddy core stations, for example, before bloom decline, $n = 4$) and 0 to 150 m at control stations ($n = 3$). Taxon-specific pigments include fucoxanthin (diatoms), chlorophyllide a (degradation pigment associated with senescent and grazed diatoms), divinyl chlorophyll a (*Prochlorococcus* spp.), and zeaxanthin (all cyanobacteria).

	Inside Opal	Outside Opal	IN/OUT or Δ
Mixed layer depth (m)	51 ± 8 m ($n = 48$)	95 ± 7 m ($n = 48$)	-
1% light level (m)	89 ± 10 m ($n = 20$)	132 ± 19 m ($n = 18$)	-
N+ N (0 to 110 m, mmol N m^{-2})	91 ± 15 ($n = 7$)^{obs}	24 ± 5 ($n = 3$)	3.8^{obs}
	147 ± 32 ($n = 3$)^{exp}		6.1^{exp}
Phosphate (0 to 110 m, mmol P m^{-2})	17.1 ± 2.5 ($n = 7$)^{obs}	9.8 ± 1.8 ($n = 3$)	1.7^{obs}
	25.9 ± 4.6 ($n = 3$)^{exp}		2.6^{exp}
Silicic acid (0 to 110 m, mmol Si m^{-2})	166 ± 30 ($n = 7$)^{obs}	170 ± 41 ($n = 3$)	1.0^{obs}
	244 ± 50 ($n = 3$)^{exp}		1.4^{exp}
TOC (0 to 110 m, mol C m^{-2})	7.26 ± 0.22 ($n = 6$)^{obs}	7.91 ± 0.03 ($n = 3$)	0.9^{obs}
	6.66 ± 0.26 ($n = 3$)^{exp}		0.8^{exp}
Si/N ratio	1.8 ± 0.5 ($n = 7$)^{obs}	7.1 ± 2.2 ($n = 3$)	
N/P ratio	5.3 ± 1.2 ($n = 7$)^{obs}	2.4 ± 0.7 (n = 3)	
PP from phytoplankton growth (mmol C m^{-2} day^{-1})	128 ± 16 ($n = 3$)	46 ± 13 ($n = 3$)	2.8
GPP from $\Delta^{17}O$ (mmol C m^{-2} day^{-1})	125 ± 6 ($n = 2$)	51 ± 27 ($n = 3$)	2.5
TChl a (mg m^{-2})	32.1 ± 4.9 ($n = 4$)	29.1 ± 1.8 ($n = 3$)	1.1
Fucoxanthin (mg m^{-2})	5.5 ± 1.6 ($n = 4$)	1.0 ± 0.02 ($n = 3$)	5.5
Chlorophyllide a (mg m^{-2})	3.2 ± 1.1 ($n = 4$)	0.2 ± 0.2 ($n = 3$)	16
Divinyl chlorophyll a (mg m^{-2})	7.6 ± 1.1 ($n = 4$)	13.7 ± 1.1 ($n = 3$)	0.6
Zeaxanthin (mg m^{-2})	5.3 ± 0.7 ($n = 4$)	9.7 ± 0.3 ($n = 3$)	0.5
Phytoplankton biomass (mmol C m^{-2})	220 ± 35 ($n = 4$)	114 ± 7 ($n = 3$)	1.9
Diatom biomass (mmol C m^{-2})	141 ± 39 ($n = 4$)	3 ± 2 ($n = 3$)	47
Prochlorococcus spp. (mmol C m^{-2})	32 ± 5 (n = 4)	58 ± 16 ($n = 3$)	0.6
Protozoan grazers (mmol C m^{-2})	78 ± 12 ($n = 4$)	59 ± 11 ($n = 3$)	1.3
Heterotrophic bacteria (mmol C m^{-2})	71 ± 7 ($n = 4$)	80 ± 7 ($n = 3$)	0.9
NCP based on dissolved inorganic C, TOC, and N+N mass balance (mmol C m^{-2} day^{-1})	14.0 ± 4.4	2.5 ± 1.9	5.6
NCP from $\Delta^{17}O$ and O_2/Ar (mmol C m^{-2} day^{-1})	6.6 ± 7.5 ($n = 2$)	2.5 ± 1.0 ($n = 3$)	2.6
PC export at 150 m (mmol m^{-2} day^{-1})			
Traps	1.54 ± 0.11 ($n = 3$)	1.52 ± 0.20 ($n = 3$)	1.0
^{15}N mass balance	2.79 ± 0.8	1.39 ± 0.46	2.0
^{234}Th derived	0.97 ± 0.57 ($n = 5$)	0.85 ± 0.08 ($n = 3$)	1.1
PN export at 150 m (mmol m^{-2} day^{-1})			
Traps	0.15 ± 0.01 ($n = 3$)	0.16 ± 0.02 ($n = 3$)	0.9
^{15}N mass balance	0.42 ± 0.13	0.21 ± 0.07	2.0
^{234}Th-derived	0.07 ± 0.04 ($n = 5$)	0.05 ± 0.01 ($n = 3$)	1.4
PSi export at 150 m (mmol m^{-2} day^{-1})			
Traps	0.427 ± 0.034 ($n = 3$)	0.111 ± 0.065 ($n = 3$)	3.8
^{234}Th-derived	0.145 ± 0.110 ($n = 5$)	0.100 ± 0.027 ($n = 2$)	1.5

Although PC export only modestly increased in Cyclone Opal, the biogenic particulate silica (PSi) flux was enhanced by 1.5 to 4 times more than fluxes at control stations, Sta. ALOHA (0.085 ± 0.058 mmol Si m^{-2} day^{-1}), and other oligotrophic open-ocean sites (e.g., Sargasso Sea, 0.107 ± 0.036 mmol Si m^{-2} day^{-1}) (*23*) (Table 1). Within the eddy, high PSi fluxes relative to PC fluxes were confirmed by visual observations of empty diatom frustules in sediment trap material and an increase in PSi/PC ratios sampled at 150 m during the time series. For comparison, these eddy-induced PSi fluxes were similar in magnitude to those observed in the more productive equatorial Pacific (~0.330 mmol Si m^{-2} day^{-1} at 200 m) and had PSi/PC molar ratios more than double those found there (*24*) and at Sta. ALOHA.

This study provides a direct biogeochemical quantification of the decline and fate of an eddy-stimulated diatom bloom in the oligotrophic open ocean. Although our results confirm that wind-driven first baroclinic mode cyclonic eddies are highly productive and increase biomass (*1*, *6*, *8*), they are not necessarily more efficient in exporting PC and PN to deep waters. The observation that eddy-enhanced production only yields a proportional increase in C export is at odds with the general perception that marked increases in the export/production ratio follow major shifts in community size structure from small to large phytoplankton (*25*, *26*). Nonetheless, the surprisingly low export efficiency in Cyclone Opal is consistent with models of temperature effects on export production (*21*), as well as warm-water diatom blooms induced by iron fertilization in the equatorial Pacific (*11*, *27*). Here, the unusual occurrence of a centric diatom bloom residing relatively deep in the euphotic zone seems to represent ideal conditions for a major flux event. The absence of disproportionate organic export fluxes under these circumstances argues that strong microbial community coupling of production, grazing, and remineralization processes in warm-water Pacific ecosystems may dampen nutrient-perturbation effects on the C export ratio.

Episodic inputs of nutrients and trace elements into surface waters by eddies, fronts, and human manipulation have been widely invoked as mechanisms that enhance C sequestration or explain regional discrepancies in nutrient and new production mass balances (*2*, *10*, *11*, *28*). Whether these speculations are reasonable for tropical and subtropical waters depends on the extent to which they incorporate community structure or production enhancement of export ratios and the temporal and spatial scales being considered. Here, the eventual decay of Cyclone Opal would have relaxed uplifted isopycnal surfaces and moved downward any unused nutrients and accumulated organic matter within

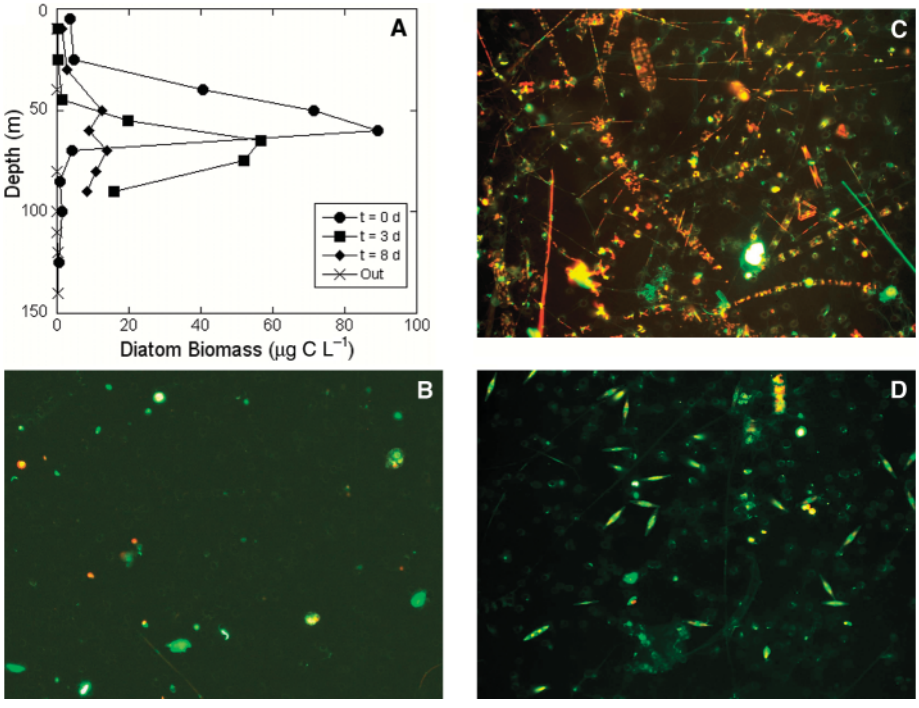

Fig. 3. Diatom biomass in the DCM. (**A**) Diatom biomass versus depth (μg C l^{-1}) during the decline of a diatom bloom; $t = 0$ (solid circles) denotes the first sampling of the bloom. Repeated samplings on days 3 and 8 after the initial encounter depicted by solid squares and diamonds, respectively. For comparison, the OUT station is also shown (crosses). (**B**) An epifluorescent image of the phytoplankton population within the DCM at the OUT station. (**C** and **D**) Epifluorescent images of the phytoplankton population within the DCM at the center of Cyclone Opal during the initial sampling [$t = 0$ day (C)] and 8 days later [$t = 8$ days (D)] during the bloom decline. Images were taken of slides viewed at 200× magnification, and each image represents >8 μm cells from 500 ml of preserved seawater (*9*). The red color reflects chlorophyll autofluorescence. Note the transition in diatom species from large centric genera (*Rhizosolenia* and *Chaetoceros*) to smaller genera (for example, *Mastogloia*).

those density layers from lighted surface waters. Thus, elemental constituents locked into eddies by efficient remineralization are exported but not effectively sequestered on annual time scales, because they reside immediately below the euphotic zone. Nonetheless, if eddies function as selective silica pumps (*14*), these sub-euphotic waters will be disproportionately depleted in silicic acid. To the extent that Si-limitation modulates diatom growth and biomass accumulation, one long-term consequence of repeated nutrient entrainment by wind-driven eddies may be to reduce diatom response, further complicating explanations of how these features affect open-ocean biogeochemistry.

References and Notes

1. R. R. Bidigare *et al.*, *Geophys. Res. Lett.* **30**, 1318 (2003).
2. D. J. McGillicuddy *et al.*, *Nature* **394**, 263 (1998).
3. A. Oschlies, *Deep-Sea Res. I* **48**, 2173 (2001).
4. W. Patzert, "Eddies in Hawaiian Islands report no. HIG-69-8" (University of Hawaii, Honolulu, 1969).
5. C. Chavanne, P. Flament, R. Lumpkin, B. Dousset, A. Bentamy, *Can. J. Remote Sensing* **28**, 466 (2002).
6. M. P. Seki *et al.*, *Geophys. Res. Lett.* **28**, 1583 (2001).
7. R. Vaillancourt, J. Marra, M. Seki, M. Parsons, R. Bidigare, *Deep-Sea Res. I* **50**, 829 (2003).
8. P. Falkowski, D. Zieman, Z. Kolber, P. Bienfang, *Nature* **352**, 55 (1991).
9. Materials and methods are available on *Science* Online.
10. K. Coale *et al.*, *Science* **304**, 408 (2004).
11. K. Coale *et al.*, *Nature* **383**, 495 (1996).
12. R. Scharek, M. Latasa, D. M. Karl, R. R. Bidigare, *Deep-Sea Res. I* **46**, 1051 (1999).
13. S. Emerson *et al.*, *Nature* **389**, 951 (1997).
14. R. Dugdale, F. Wilkerson, H. Minas, *Deep-Sea Res. I* **42**, 697 (1995).
15. S. J. Giovannoni, M. S. Rappé, in *Microbial Ecology of the Oceans*, D. L. Kirchman, Ed. (Wiley-Liss, New York, 2000), p. 47.
16. E. F. DeLong, D. G. Franks, A. L. Alldredge, *Limnol. Oceanogr.* **38**, 924 (1993).
17. H. Reichenbach, in *The Prokaryotes*, A. Barlows, Ed. (Springer-Verlag, New York, 1992), p. 3631.
18. C. R. Benitez-Nelson, K. O. Buesseler, D. M. Karl, J. Andrews, *Deep-Sea Res. I* **48**, 2595 (2001).
19. L. W. Juranek, P. D. Quay, *Global Biogeochem. Cycles* **19**, 10.1029/2004GB002384 (2005).
20. R. Eppley, B. Peterson, *Nature* **282**, 677 (1979).
21. E. A. Laws, P. G. Falkowski, W. O. Smith, H. Ducklow, J. J. McCarthy, *Global Biogeochem. Cycles* **14**, 1231 (2000).
22. K. O. Buesseler, *Global Biogeochem. Cycles* **12**, 297 (1998).
23. D. Nelson, M. Brzezinski, *Limnol. Oceanogr.* **42**, 473 (1997).
24. O. Ragueneau, N. Dittert, P. Pondaven, P. Tréguer, L. Corrin, *Deep-Sea Res. II* **49**, 3127 (2002).
25. A. F. Michaels, M. W. Silver, *Deep-Sea Res.* **35**, 473 (1988).
26. P. Boyd, P. Newton, *Deep-Sea Res. I* **46**, 63 (1999).
27. M. Landry *et al.*, *Mar. Ecol. Prog. Ser.* **201**, 57 (2000).
28. C. Sakamoto *et al.*, *J. Geophys. Res.* **109**, 10.1029/2003JC001976 (2004).
29. A. Morel, *J. Geophys. Res.* **93**, 10749 (1988).

30. Our sincere thanks are due to R. R. Bidigare III and R. Styles for help with sample collection and analyses; D. M. Karl, P. Falkowski, and M. Gorbunov for equipment and allowing their students and postdoctoral fellows to participate; and the captain and crew of the R/V *Wecoma*. This research was supported by the Ocean Sciences Division of the NSF. P.M. was supported by a grant from the Gordon and Betty Moore Foundation.

Supporting Online Material

www.sciencemag.org/cgi/content/full/316/5827/1017/DC1
Materials and Methods
References

12 October 2006; accepted 26 March 2007
10.1126/science.1136221

Eddy/Wind Interactions Stimulate Extraordinary Mid-Ocean Plankton Blooms

Dennis J. McGillicuddy Jr.,[1]* Laurence A. Anderson,[1] Nicholas R. Bates,[2] Thomas Bibby,[3,4] Ken O. Buesseler,[1] Craig A. Carlson,[5] Cabell S. Davis,[1] Courtney Ewart,[5] Paul G. Falkowski,[3] Sarah A. Goldthwait,[6,7] Dennis A. Hansell,[8] William J. Jenkins,[1] Rodney Johnson,[2] Valery K. Kosnyrev,[1] James R. Ledwell,[1] Qian P. Li,[8] David A. Siegel,[5] Deborah K. Steinberg[6]

Episodic eddy-driven upwelling may supply a significant fraction of the nutrients required to sustain primary productivity of the subtropical ocean. New observations in the northwest Atlantic reveal that, although plankton blooms occur in both cyclones and mode-water eddies, the biological responses differ. Mode-water eddies can generate extraordinary diatom biomass and primary production at depth, relative to the time series near Bermuda. These blooms are sustained by eddy/wind interactions, which amplify the eddy-induced upwelling. In contrast, eddy/wind interactions dampen eddy-induced upwelling in cyclones. Carbon export inferred from oxygen anomalies in eddy cores is one to three times as much as annual new production for the region.

Understanding the controls on primary production in the upper ocean is of fundamental importance for two main reasons. First, primary productivity sets a first-order constraint on the energy available to sustain oceanic ecosystems. Second, fixation and subsequent sinking of organic particles remove carbon from the surface ocean (the so-called biological